

# Electronic Supporting Information

## Boosting Purely Organic Room-Temperature Phosphorescence Performance through Host-Guest Strategy

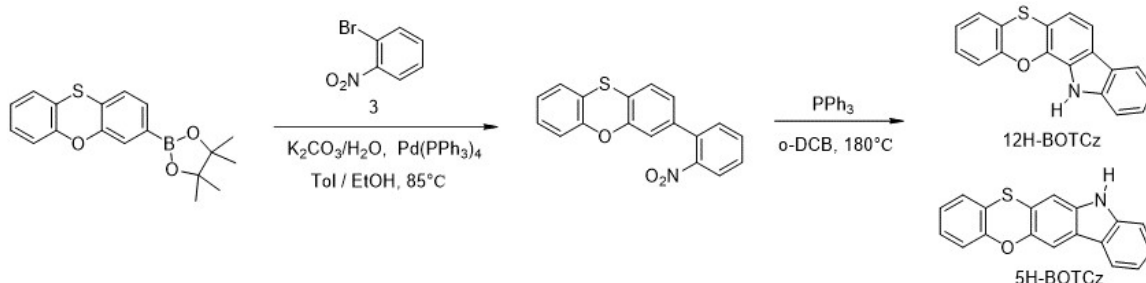
Mengke Li,<sup>a</sup> Xinyi Cai,<sup>a</sup> Zijian Chen,<sup>a</sup> Kunkun Liu,<sup>a,b</sup> Weidong Qiu,<sup>a</sup> Wentao Xie,<sup>a</sup> Liangying Wang<sup>a</sup> and Shi-Jian Su<sup>\*a,b</sup>

<sup>a</sup> State Key Laboratory of Luminescent Materials and Devices and Institute of Polymer Optoelectronic Materials and Devices, South China University of Technology, Guangzhou 510640, P. R. China.

<sup>b</sup> South China Institute of Collaborative Innovation, Dongguan 523808, China.

### 1. Materials and Synthesis Procedures

#### Synthesis of 12H-BOTCz and 5H-BOTCz



4,4,5,5-Tetramethyl-2-(phenoxathiin-3-yl)-1,3,2-dioxaborolane (2.58 g, 7.9 mmol), 1-bromo-2-nitrobenzene (1.45 g, 7.2 mmol), and  $K_2CO_3$  (2.18 g, 15.8 mmol) was added to a 150 mL three-necked flask with mixture solution of THF (60 mL) and  $H_2O$  (30 mL). The mixture was heated to  $110^\circ C$  and stirred for 12 hours under  $N_2$  atmosphere. The resultant was extracted with dichloromethane, drying with anhydrous magnesium sulfate and further purified by column chromatography to obtain faint yellow solid (1.9 g, 75%). Then, the resultant compound **3** (1.9 g, 5.9 mmol) and triphenylphosphane (4.64 g, 17.7 mmol) were dissolved in *o*-DCB (15 mL) under and added to a 50 mL three-necked flask. The mixture was added to  $200^\circ C$  under  $N_2$  atmosphere and stirred for 36 hours. The resultant was directly purified by column chromatography to give white solid PXTCz1 (427 mg, 25%) and PXTCz2 (342 mg, 20%) simultaneously.

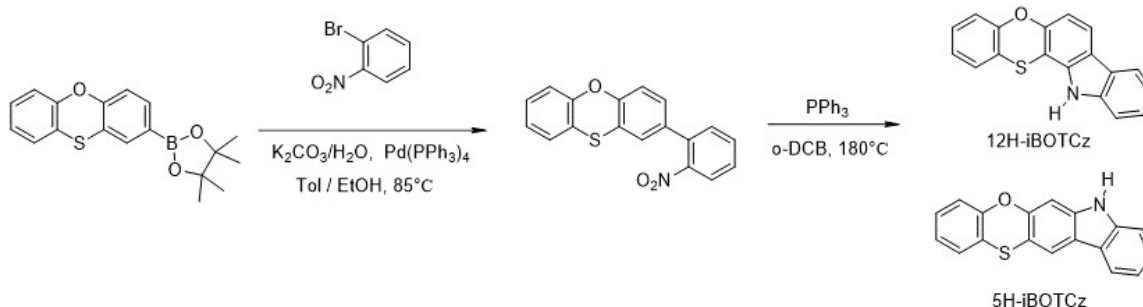
**12H-BOTCz:**  $^1H$  NMR (500 MHz,  $DMSO-d_6$ )  $\delta$  11.62 (s, 1H), 8.09 (d,  $J = 7.7$  Hz, 1H), 7.86 (d,  $J = 8.1$  Hz, 1H), 7.54 (d,  $J = 8.1$  Hz, 1H), 7.47 – 7.39 (m, 1H), 7.37 – 7.27 (m, 2H), 7.24 (dd,  $J = 8.0, 1.5$  Hz, 1H), 7.21 – 7.11 (m, 2H), 6.97 (d,  $J = 8.1$  Hz, 1H).  $^{13}C$  NMR (126 MHz,  $DMSO-d_6$ )  $\delta$  152.08, 140.42, 137.18, 129.84, 128.77, 127.72, 126.53, 125.62, 124.47, 122.87, 120.83, 120.49,

119.70, 118.19, 117.17, 117.11, 114.58, 111.99. Calcd (C<sub>18</sub>H<sub>11</sub>N<sub>1</sub>O<sub>1</sub>S<sub>1</sub>): 289.35, APCI-MS (mass m/z); found: 290.15 ((M+1)+).

**5H-BOTCz:** <sup>1</sup>H NMR (500 MHz, DMSO-*d*<sub>6</sub>) δ 11.23 (s, 1H), 8.10 (d, *J* = 7.8 Hz, 1H), 7.94 (s, 1H), 7.46 (d, *J* = 8.1 Hz, 1H), 7.43 – 7.35 (m, 2H), 7.33 (dd, *J* = 7.8, 1.6 Hz, 1H), 7.26 (td, *J* = 7.7, 1.6 Hz, 1H), 7.21 – 7.06 (m, 3H). <sup>13</sup>C NMR (126 MHz, DMSO-*d*<sub>6</sub>) δ 153.17, 145.52, 141.02, 137.36, 130.11, 128.65, 127.43, 126.49, 125.11, 122.59, 122.48, 120.95, 120.85, 119.16, 118.21, 111.65, 109.12, 108.76. Calcd (C<sub>18</sub>H<sub>11</sub>N<sub>1</sub>O<sub>1</sub>S<sub>1</sub>): 289.35, APCI-MS (mass m/z); found: 290.23 ((M+1)+).

### Synthesis of 12H-iBOTCz and 5H-iBOTCz

These two compounds were synthesized in the similar way with compounds 12H-BOTCz and 5H-BOTCz by replacing 4,4,5,5-tetramethyl-2-(phenoxathiin-3-yl)-1,3,2-dioxaborolane (2.58 g, 7.9 mmol) with 4,4,5,5-tetramethyl-2-(phenoxathiin-2-yl)-1,3,2-dioxaborolane (2.58 g, 7.9 mmol).

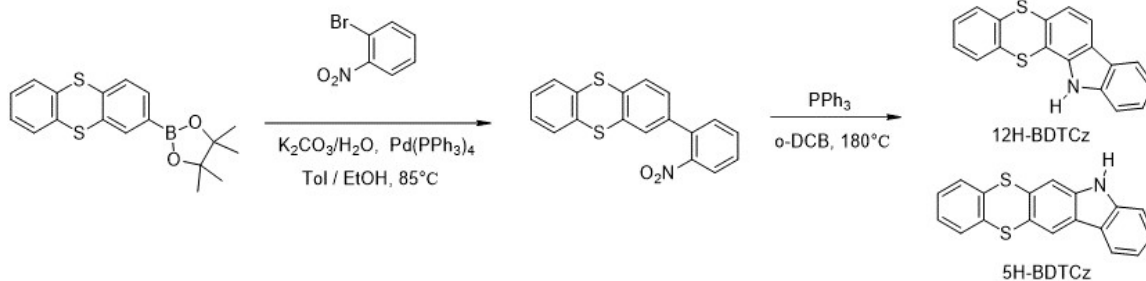


**12H-iBOTCz:** <sup>1</sup>H NMR (400 MHz, DMSO-*d*<sub>6</sub>) δ 11.44 (s, 1H), 8.07 (d, *J* = 7.8 Hz, 1H), 7.97 (d, *J* = 8.4 Hz, 1H), 7.51 (d, *J* = 8.1 Hz, 1H), 7.38 (ddd, *J* = 8.0, 4.4, 1.6 Hz, 2H), 7.28 (ddd, *J* = 8.5, 7.2, 1.6 Hz, 1H), 7.22 – 7.10 (m, 3H), 6.97 (d, *J* = 8.4 Hz, 1H). <sup>13</sup>C NMR (126 MHz, DMSO-*d*<sub>6</sub>) δ 152.48, 150.13, 140.84, 136.74, 128.96, 127.79, 125.88, 125.51, 122.79, 120.54, 120.17, 119.87, 119.71, 118.99, 118.49, 111.85, 109.93, 100.96. Calcd (C<sub>18</sub>H<sub>11</sub>N<sub>1</sub>O<sub>1</sub>S<sub>1</sub>): 289.35, APCI-MS (mass m/z); found: 290.15 ((M+1)+).

**5H-iBOTCz:** <sup>1</sup>H NMR (400 MHz, DMSO-*d*<sub>6</sub>) δ 11.33 (s, 1H), 8.19 – 7.90 (m, 2H), 7.46 (d, *J* = 8.1 Hz, 1H), 7.39 – 7.30 (m, 2H), 7.28 – 7.22 (m, 2H), 7.19 (d, *J* = 1.4 Hz, 1H), 7.18 – 7.09 (m, 2H). <sup>13</sup>C NMR (126 MHz, DMSO-*d*<sub>6</sub>) δ 152.67, 150.96, 140.74, 140.03, 128.47, 127.45, 125.95, 125.33, 122.05, 121.45, 120.60, 120.49, 119.48, 118.54, 118.29, 111.50, 109.88, 100.60. Calcd (C<sub>18</sub>H<sub>11</sub>N<sub>1</sub>O<sub>1</sub>S<sub>1</sub>): 289.35, APCI-MS (mass m/z); found: 290.23 ((M+1)+).

### Synthesis of 12H-BDTCz and 5H-BDTCz

These two compounds were synthesized in the similar way with compounds 12H-BOTCz and 5H-BOTCz by replacing 4,4,5,5-tetramethyl-2-(phenoxathiin-3-yl)-1,3,2-dioxaborolane (2.58 g, 7.9 mmol) with 4,4,5,5-tetramethyl-2-(thianthren-2-yl)-1,3,2-dioxaborolane (2.70 g, 7.9 mmol).



**12H-BDTCz:**  $^1\text{H}$  NMR (400 MHz,  $\text{DMSO}-d_6$ )  $\delta$  11.61 (s, 1H), 8.12 (t,  $J = 7.4$  Hz, 2H), 7.76 – 7.62 (m, 2H), 7.58 (d,  $J = 8.1$  Hz, 1H), 7.50 – 7.30 (m, 4H), 7.20 (t,  $J = 7.4$  Hz, 1H).  $^{13}\text{C}$  NMR (126 MHz,  $\text{DMSO}-d_6$ )  $\delta$  140.50, 138.49, 136.32, 134.60, 131.74, 129.45, 129.35, 128.81, 128.70, 126.72, 122.93, 122.69, 121.02, 120.33, 119.93, 119.83, 116.25, 112.14. Calcd ( $\text{C}_{18}\text{H}_{11}\text{N}_1\text{S}_2$ ): 305.41, APCI-MS (mass  $m/z$ ); found: 306.22 ((M+1)+).

**5H-BDTCz:**  $^1\text{H}$  NMR (400 MHz,  $\text{DMSO}-d_6$ )  $\delta$  11.43 (s, 1H), 8.39 (s, 1H), 8.16 (d,  $J = 7.8$  Hz, 1H), 7.72 (s, 1H), 7.69 – 7.60 (m, 2H), 7.50 (d,  $J = 8.1$  Hz, 1H), 7.46 – 7.32 (m, 3H), 7.18 (t,  $J = 7.4$  Hz, 1H).  $^{13}\text{C}$  NMR (126 MHz,  $\text{DMSO}-d_6$ )  $\delta$  140.49, 139.99, 136.66, 134.79, 129.66, 129.53, 129.21, 128.79, 128.53, 126.71, 126.26, 123.55, 123.24, 121.68, 121.23, 119.66, 111.76, 111.25. Calcd ( $\text{C}_{18}\text{H}_{11}\text{N}_1\text{S}_2$ ): 305.41, APCI-MS (mass  $m/z$ ); found: 306.22 ((M+1)+).

## 2. Photophysical Characterization

### General information:

Steady state photoluminescence (PL) and phosphorescence spectra at ambient temperature were recorded using FluoroMax-4 spectrofluorometer. PL quantum yields (PLQYs) of all crystals were measured with HAMAMATSU absolute PL quantum yield spectrometer (C11347). Transient PL lifetimes of the powder samples were measured using Quantaaurus-Tau fluorescence lifetime measurement system (C11367-03, Hamamatsu Photonics Co., Japan). Transient PL spectra of all crystalline samples were measured with a transient lifetime spectrometer (FL980, Edinburgh Instrument). Temperature-dependent PL spectra of all crystals were recorded under Ar atmosphere using a transient lifetime spectrometer (FL980, Edinburgh Instrument).

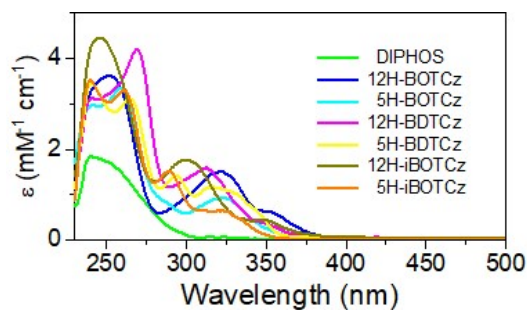


**Fig. S1** UV-vis absorption spectra of the host and guests in diluted chloroform solutions.

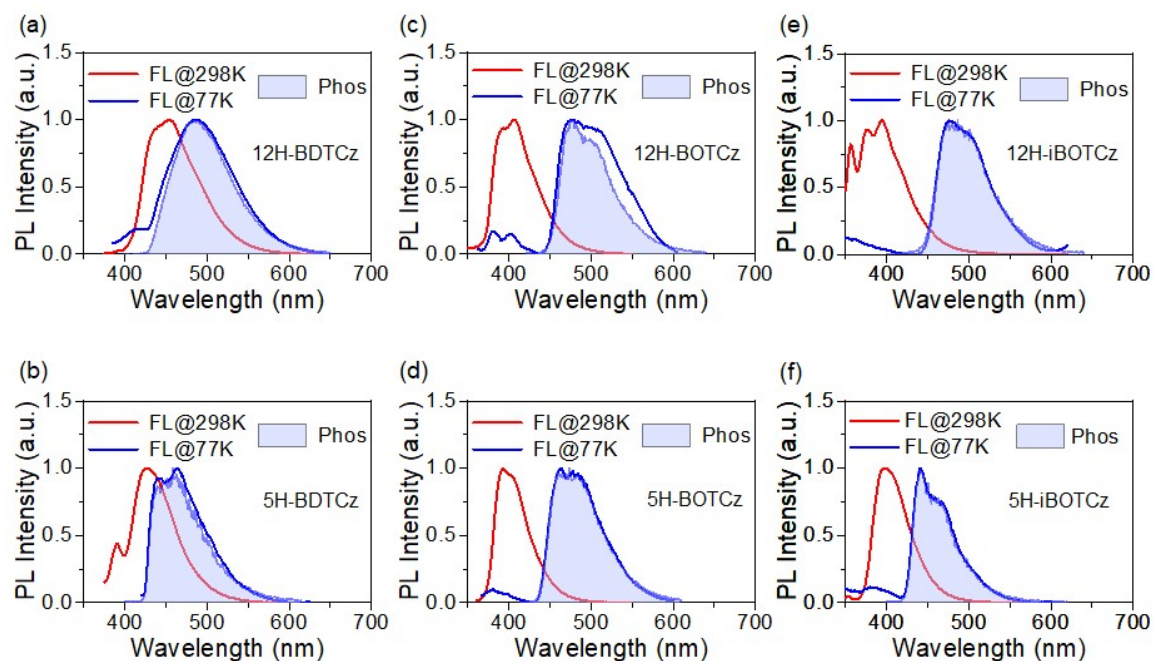


**Fig. S2** Steady state PL spectra detected at 298 K (red line) and 77 K (blue line), and low temperature phosphorescence spectra (blue area) of (a) 12H-BDTCz, (b) 5H-BDTCz, (c) 12H-BOTCz, (d) 5H-BOTCz, (e) 12H-iBOTCz and (f) 5H-iBOTCz detected in diluted toluene solutions (“FL” means fluorescence and “Phos” means phosphorescence).

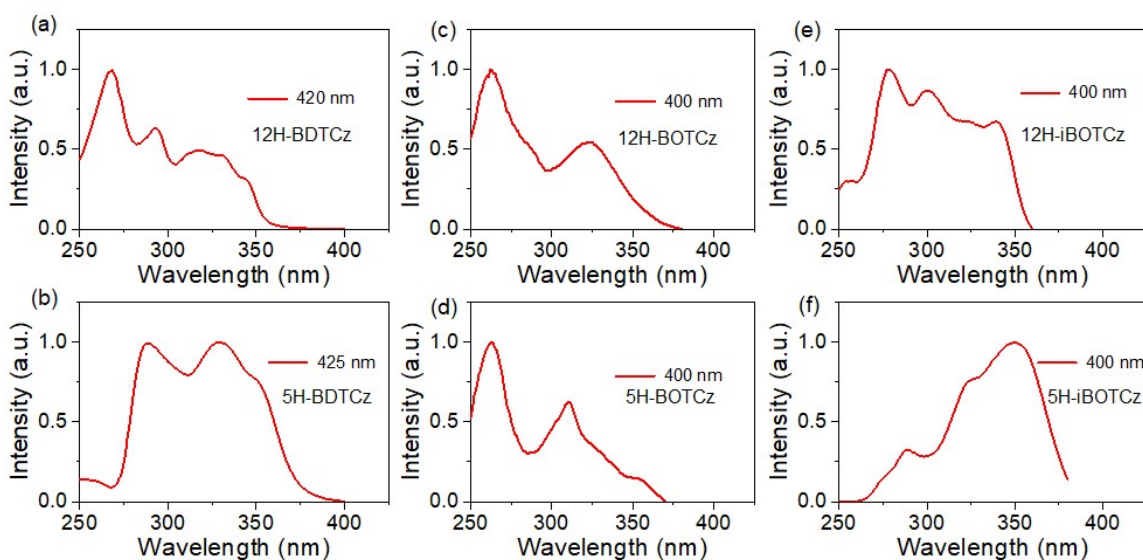


**Fig. S3** Fluorescence excitation spectra of (a) 12H-BDTCz; (b) 5H-BDTCz; (c) 12H-BOTCz; (d) 5H-BOTCz; (e) 12H-iBOTCz and (f) 5H-iBOTCz in diluted chloroform solutions.

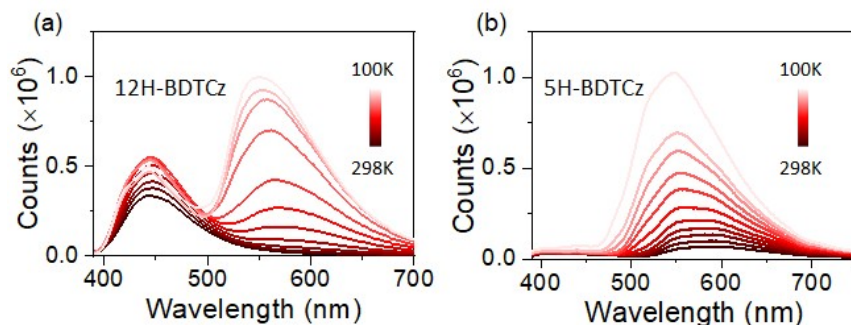


**Fig. S4** Temperature-dependent PL spectra of (a) 12H-BDTCz and (b) 5H-BDTCz in crystal states.

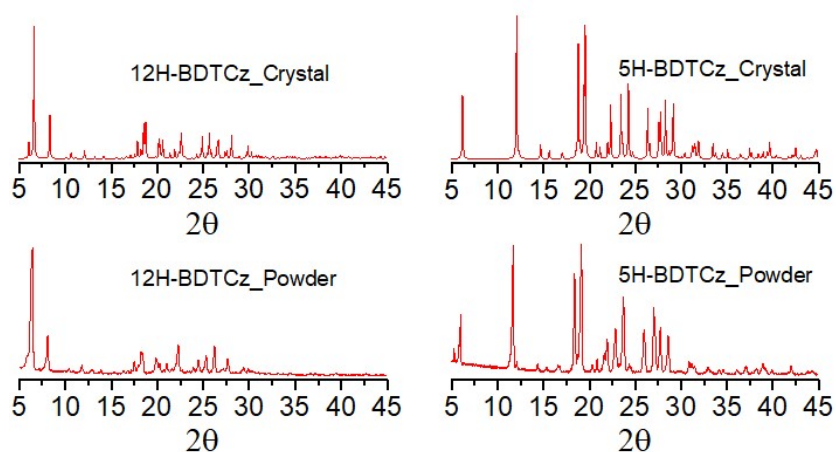


**Fig. S5** Comparison of X-ray diffraction patterns of 12H-BDTCz and 5H-BDTCz in crystal and powder states.

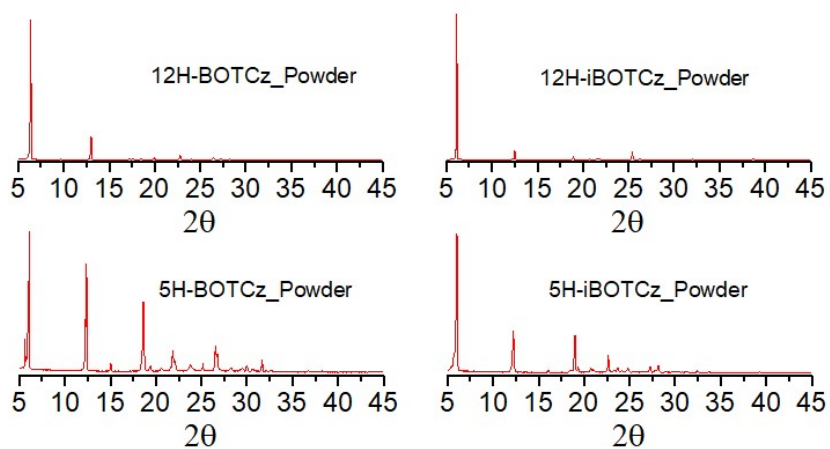


**Fig. S6** X-ray diffraction patterns of 12H-BOTCz, 5H-BOTCz, 12H-iBOTCz and 5H-iBOTCz in powder states.

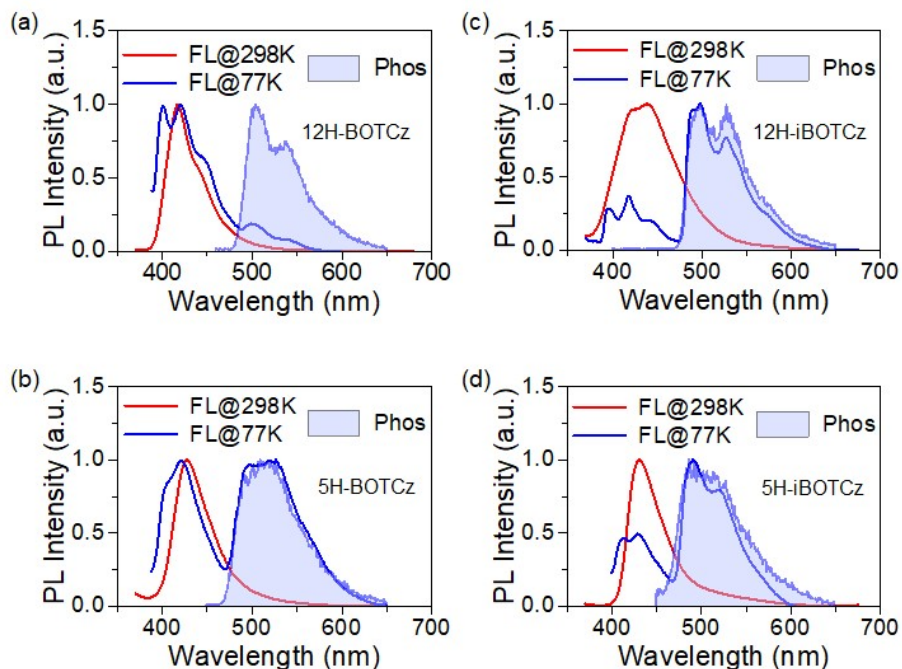


**Fig. S7** PL spectra of (a) 12H-BOTCz, (b) 5H-BOTCz, (c) 12H-iBOTCz and (d) 5H-iBOTCz in powder states detected at 298 K and 77 K, and low temperature phosphorescence spectra at 77 K with 5 ms delay.

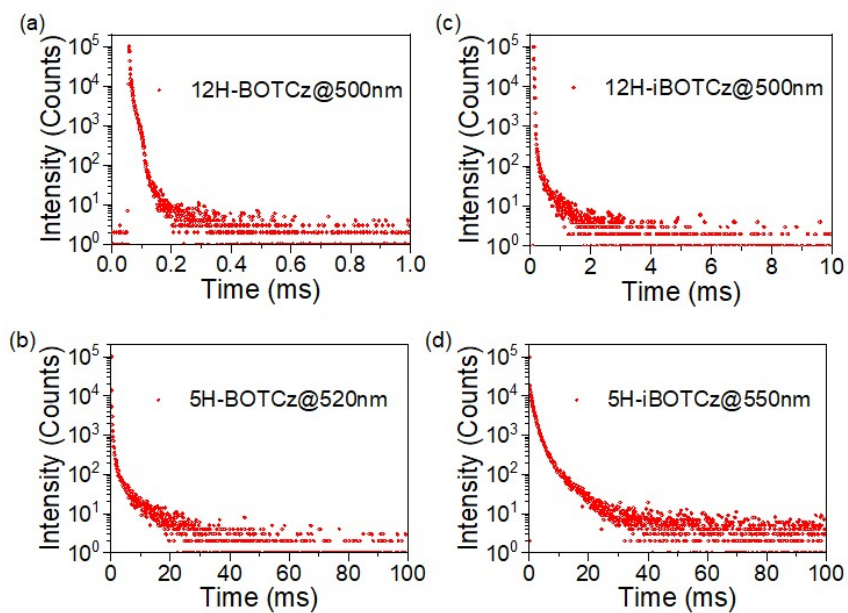


**Fig. S8** Phosphorescence decay spectra of (a) 12H-BOTCz, (b) 5H-BOTCz, (c) 12H-iBOTCz and (d) 5H-iBOTCz in powder states.

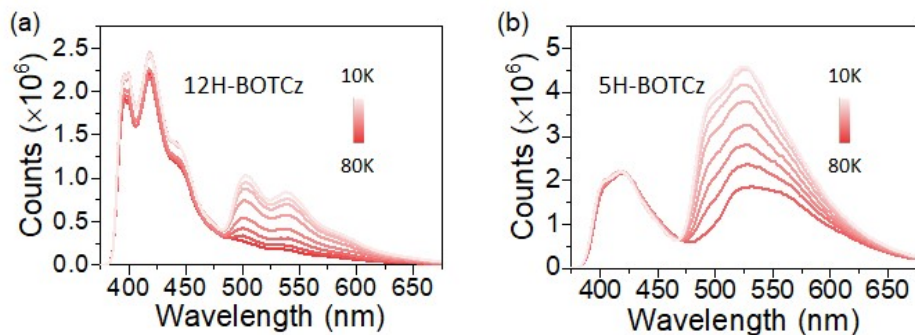


**Fig. S9** Temperature-dependent PL spectra of (a) 12H-BOTCz and (b) 5H-BOTCz in solid states.

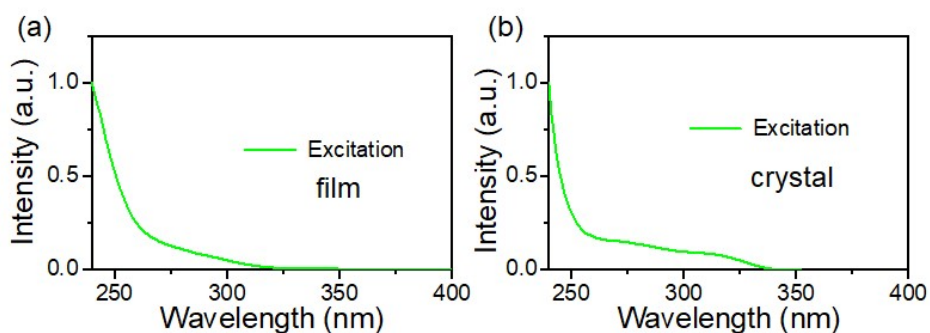


**Fig. S10** (a) Excitation spectra of the neat film of the host detected at 450 nm; (b) Excitation spectra of the host in crystal state detected at 450 nm.

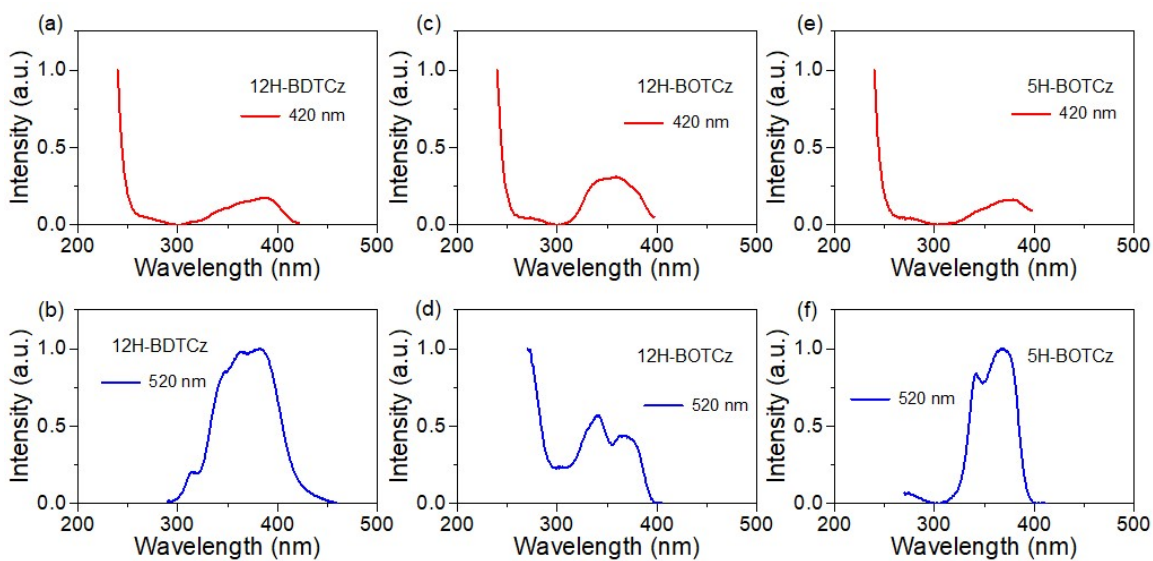


**Fig. S11** Fluorescence excitation spectra of host-guest cocrystals. (a) 12H-BOTCz: DIPHOS; (c) 12H-BOTCz: DIPHOS; (e) 5H-BOTCz: DIPHOS; And phosphorescence excitation spectra of (b) 12H-BOTCz: DIPHOS; (d) 12H-BOTCz: DIPHOS; (f) 5H-BOTCz: DIPHOS.

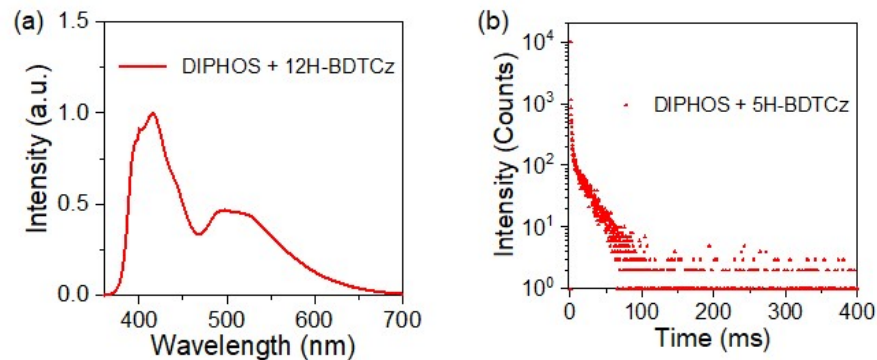


**Fig. S12** Steady state photoluminescence spectra (a) and phosphorescence decay curves (b) detected at 298 K by dissolving 12H-BDTCz into the host matrix.

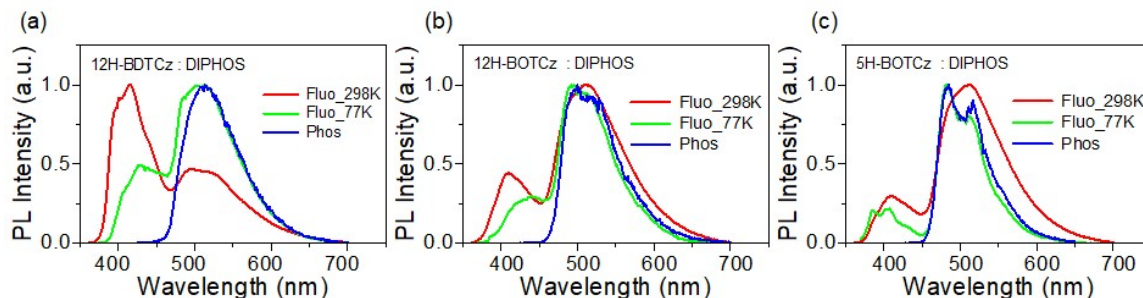


**Fig. S13** Steady-state PL spectra and phosphorescence spectra of the host-guest cocrystals: (a) 12H-BDTCz: DIPHOS; (b) 12H-BOTCz: DIPHOS and (c) 5H-BOTCz: DIPHOS. (Phosphorescence spectra were recorded at 77 K with 1 ms time delay)

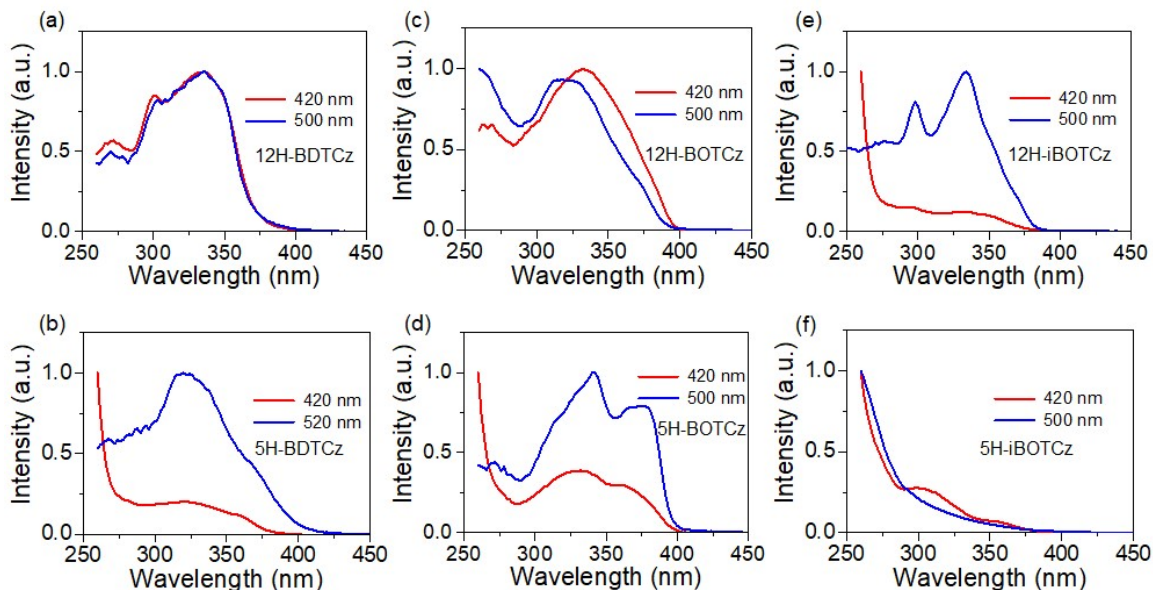


**Fig. 14** Fluorescence and phosphorescence excitation spectra of host-guest doped films of (a)

12H-BDTCz: DIPHOS; (b) 5H-BDTCz: DIPHOS; (c) 12H-BOTCz: DIPHOS; (d) 5H-BOTCz: DIPHOS; (e) 12H-iBOTCz: DIPHOS and (f) 5H-iBOTCz: DIPHOS.

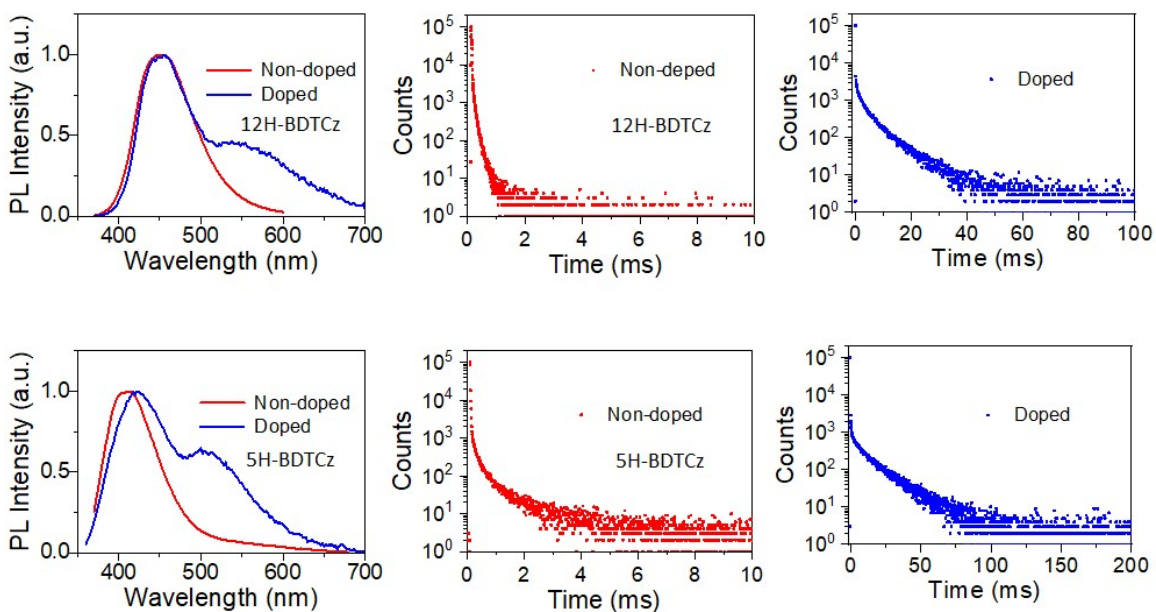


**Fig. S15** Steady-state PL spectra of (a) 12H-BDTCz and (b) 5H-BDTCz in doped and non-doped films; Phosphorescence decay curves of (c) 12H-BDTCz and (d) 5H-BDTCz in non-doped films and phosphorescence decay curves of (e) 12H-BDTCz and (f) 5H-BDTCz in doped films (“Non-doped” means neat film of the guest and “Doped” means host-guest doped film).

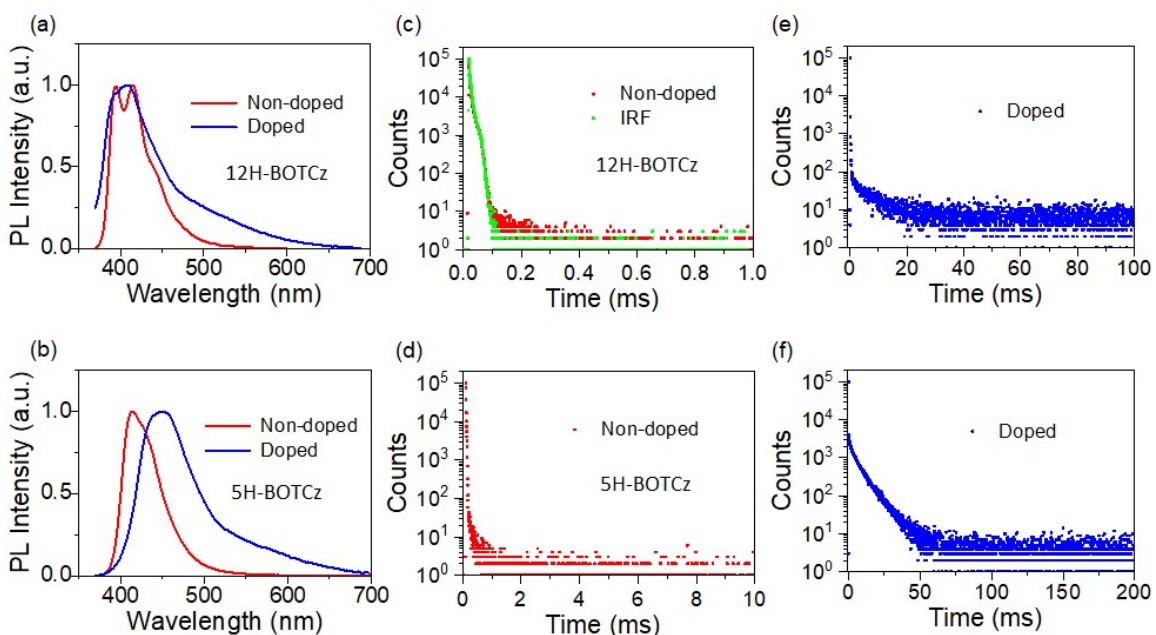


**Fig. S16** Steady-state PL spectra of (a) 12H-BOTCz and (b) 5H-BOTCz in doped and non-doped films; Phosphorescence decay curves of (c) 12H-BOTCz and (d) 5H-BOTCz in non-doped films and phosphorescence decay curves of (e) 12H-BOTCz and (f) 5H-BOTCz in doped films (“Non-doped” means neat film of the guest and “Doped” means host-guest doped film).

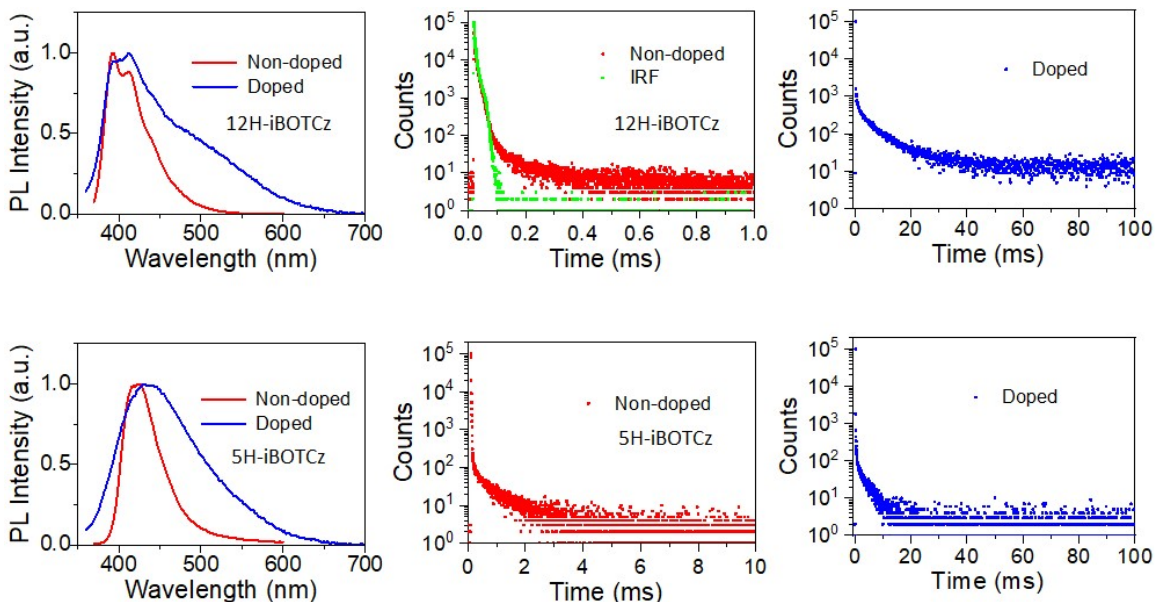


**Fig. S17** Steady-state PL spectra of (a) 12H-iBOTCz and (b) 5H-iBOTCz in doped and non-doped films; Phosphorescence decay curves of (c) 12H-iBOTCz and (d) 5H-iBOTCz in non-doped films and phosphorescence decay curves of (e) 12H-iBOTCz and (f) 5H-iBOTCz in doped films (“Non-doped” means neat film of the guest and “Doped” means host-guest doped film).

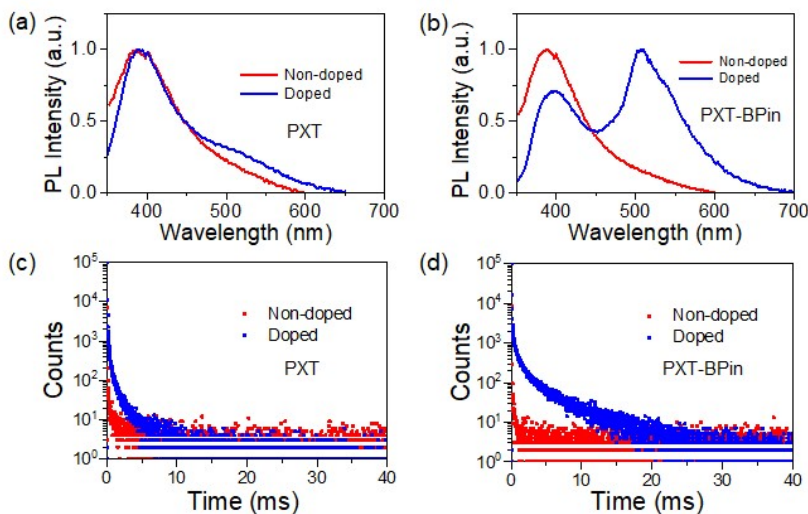


**Fig. S18** Steady-state PL spectra of (a) PXT and (c) PXT-BPin in doped and non-doped films; Phosphorescence decay curves of (b) PXT and (d) PXT-BPin in doped and non-doped films. (In the doped films, the doping concentration of the guest is 5 wt%)

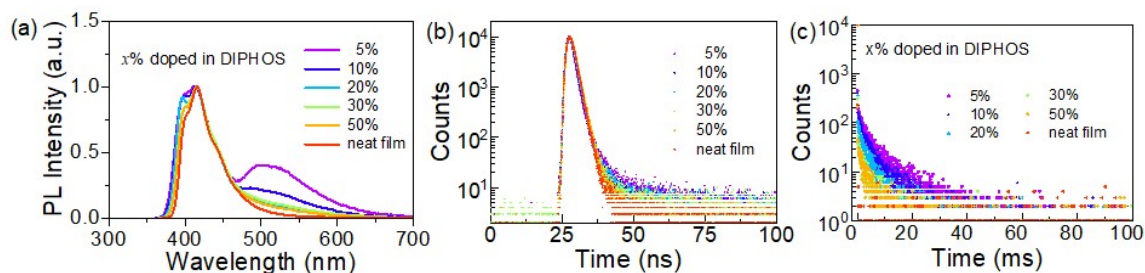


**Fig. S19** (a) Steady-state PL spectra of 12H-BOTCz doped host-guest films with different doping concentrations. (b) Fluorescence decay spectra of host-guest doped films detected at 420 nm; (c) Phosphorescence decay spectra of host-guest doped films detected at 500 nm.

### 3. Theoretical Calculation

#### 3.1 Quantum chemistry calculation

All of the quantum chemistry simulations were performed using the Gaussian 09\_E01 program package. The ground state and excited state geometries of all monomers were optimized using M06-2X functional with TZVP basis set in vacuum, and the vibrational frequencies were further calculated based on the optimized structures to confirm that the local minima were found.

For the clustered structures of crystals, a two-layer ONIOM model was adapted to perform hybrid QM/MM calculation.<sup>1</sup> The central QM part is described with quantum mechanics, whereas the surrounding MM part is treated using molecular force field (universal force field). The ground states and excited states geometries of the central QM part were optimized using M06-2X functional with TZVP basis set. The excitation energies of the singlet excited states ( $S_1$ ) and n-th triplet excited states ( $T_n$ ) were calculated with TD-DFT method based on the optimized geometries. The SOC constants between  $S_1$  and  $T_n$  were calculated using Dalton package using atomic mean field approximation approach.<sup>2</sup>

#### 3.2 Molecular dynamics (MD) simulations

All MD simulations were performed with GROMACS software package version 2019.3 using general amber force field (GAFF) and restrained electrostatic potential (RESP) atomic charge.<sup>3-5</sup> Host and guest molecules were randomly paced into a cubic box followed by a periodic annealing MD process of 100-ns under NPT ensemble. A cutoff of 1.2 nm was used to calculate non-bonded interactions in the simulations. For the final obtained aggregate host-guest cluster configurations, a two-layer ONIOM model was adapted to perform hybrid QM/MM calculation. The theoretical method of QM/MM calculation was kept consistent with the calculation of crystal structures.

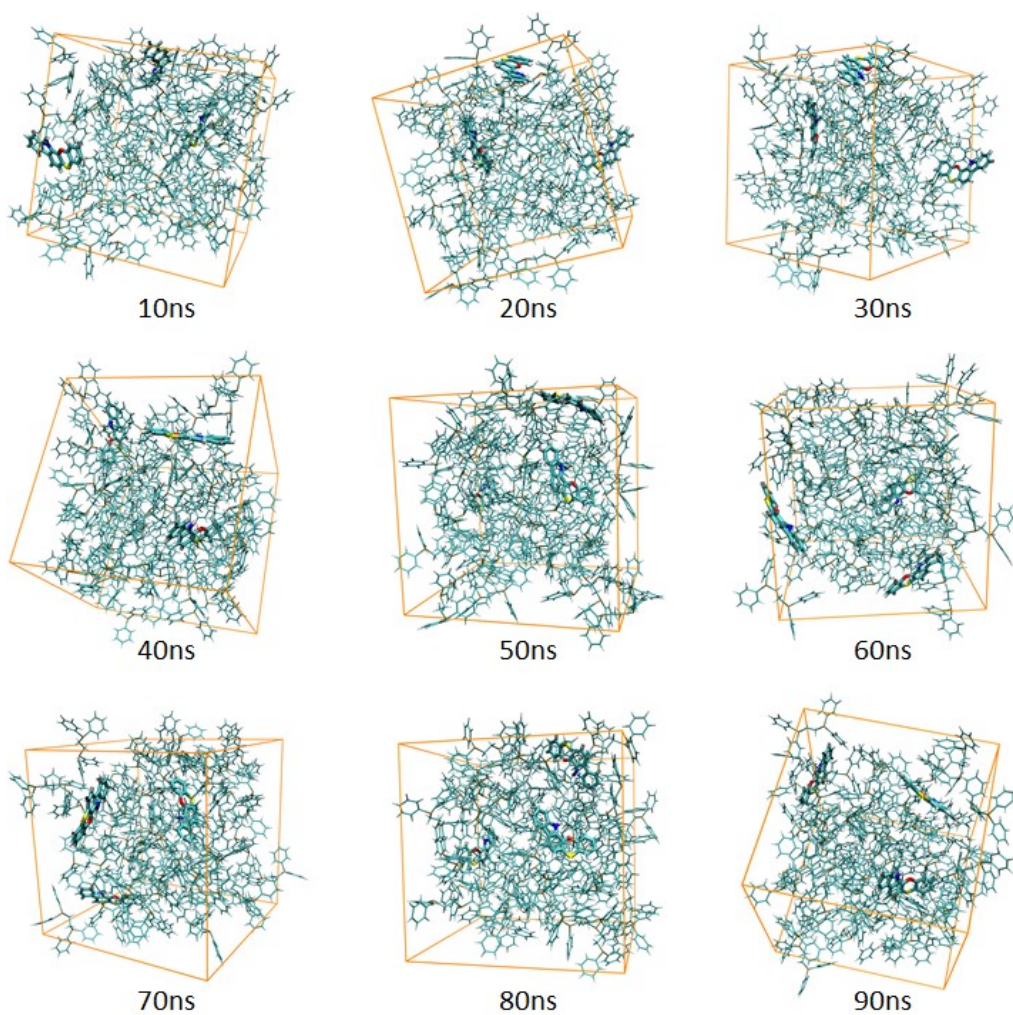


**Fig. S20** Snapshots of 12H-BOTCz/DIPHOS host-guest clusters simulated by molecular dynamics (The coarse lines represent guest molecular structures, and the thin lines represent host molecular structures).

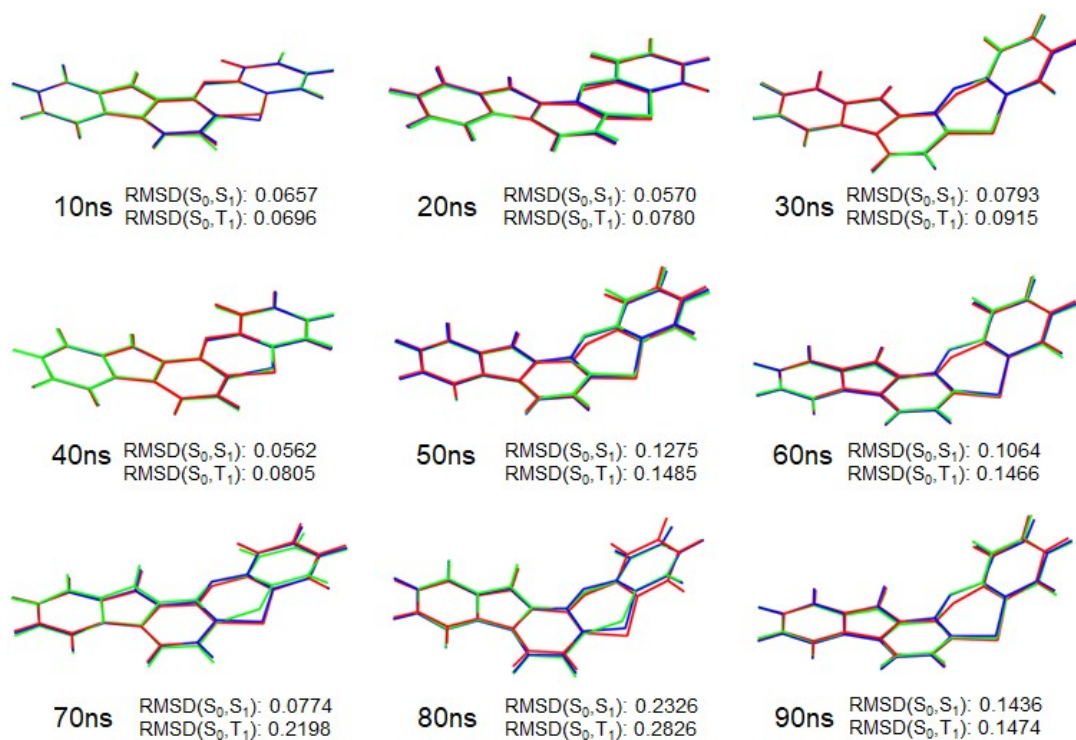


**Fig. S21** Comparison of ground states and excited states geometries of several typical clusters simulated by MD (red lines for ground state, green lines for the lowest singlet excited states and blue lines for the lowest triplet excited states).

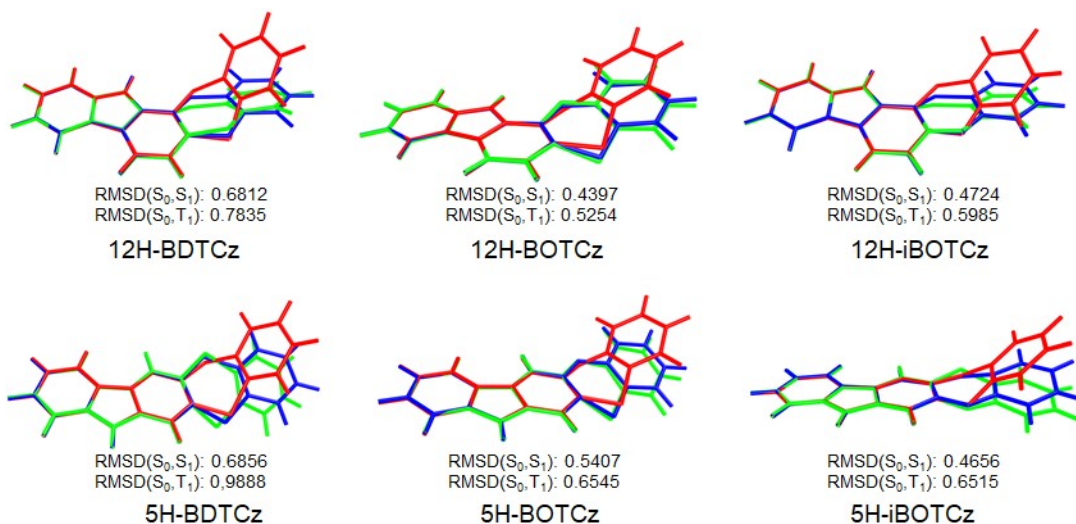


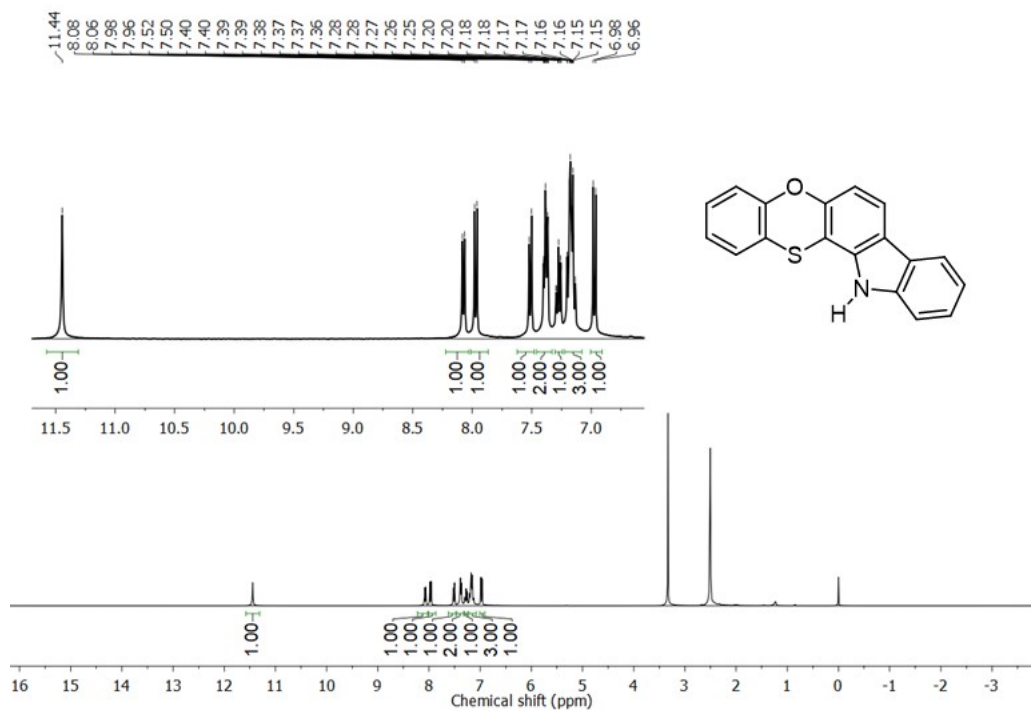
**Fig. S22** Comparison of ground states and excited states geometries of monomers (red lines for ground state, green lines for the lowest singlet excited states and blue lines for the lowest triplet excited states).

## 4. Single Crystals Information

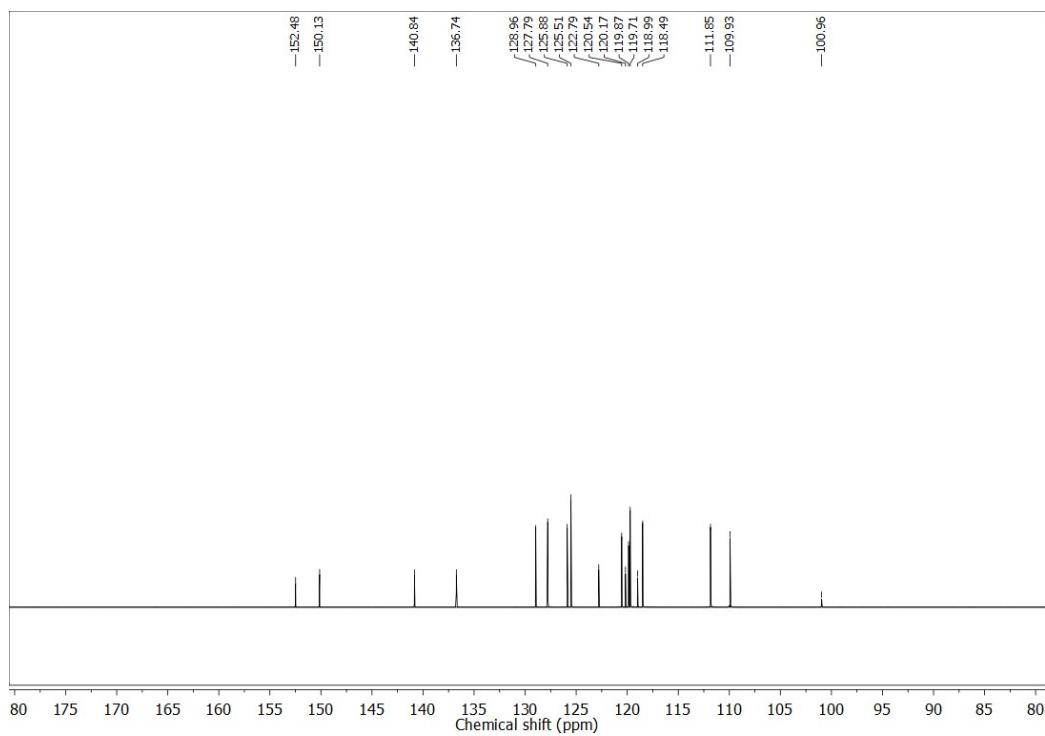
**Table S1.** Detailed information of 12H-BDTCz, 5H-BDTCz and DIPHOS single crystals.

<b>Compound</b>	<b>12H-BDTCz</b>	<b>5H-BDTCz</b>	<b>DIPHOS</b>
Formula	C <sub>18</sub> H <sub>11</sub> NS <sub>2</sub>	C <sub>18</sub> H <sub>11</sub> NS <sub>2</sub>	C <sub>26</sub> H <sub>24</sub> P <sub>2</sub>
Space Group	P 2 <sub>1</sub> /c	P 2 <sub>1</sub> 2 <sub>1</sub> 2 <sub>1</sub>	P 2 <sub>1</sub> /n
Cell Lengths (Å)	a 6.0245 b 26.7814 c 17.4898	a 6.1703 b 7.5854 c 28.6310	a 13.0545 b 5.4535 c 16.1555
Cell Angles (°)	α 90 β 92.341 γ 90	α 90 β 90 γ 90	α 90 β 111.028 γ 90
Cell Volume (Å <sup>3</sup> )	2819.53	1340.05	1073.56
Z	8	4	2

## 5. NMR Spectra



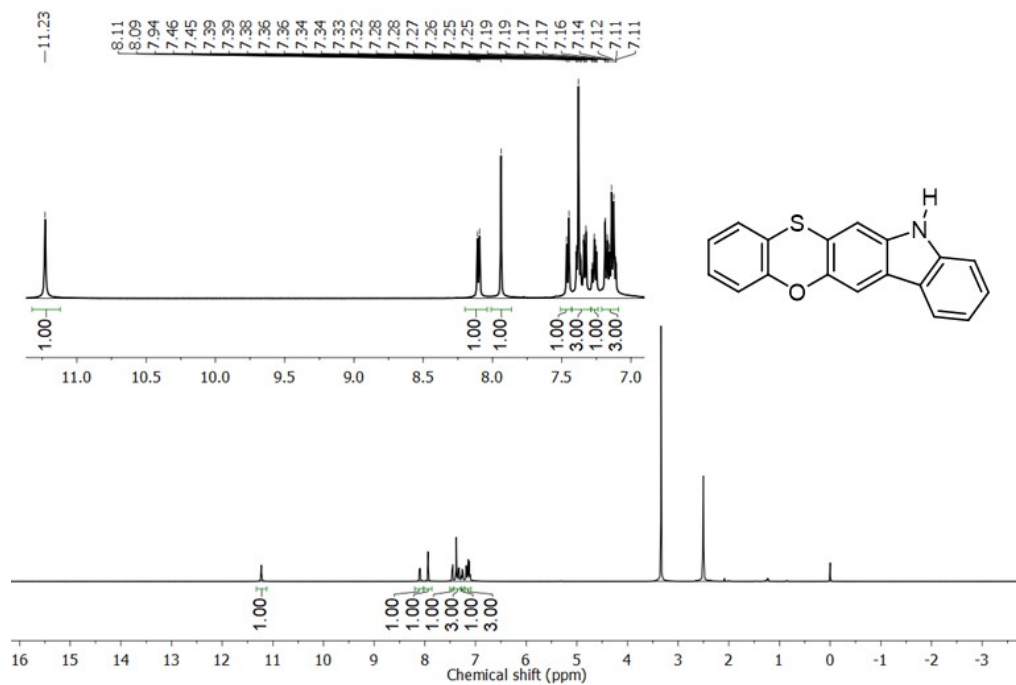
a) <sup>1</sup>H NMR spectrum of 12H-iBOTCz in deuterated DMSO solvent.



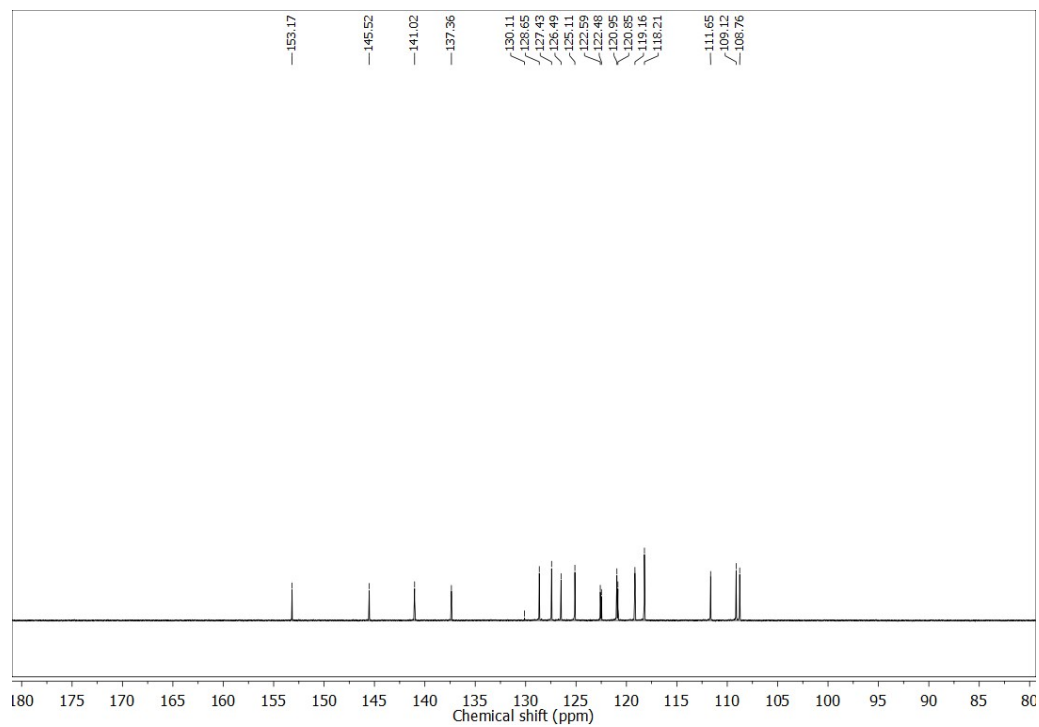
b) <sup>13</sup>C NMR spectrum of 12H-iBOTCz in deuterated DMSO solvent.



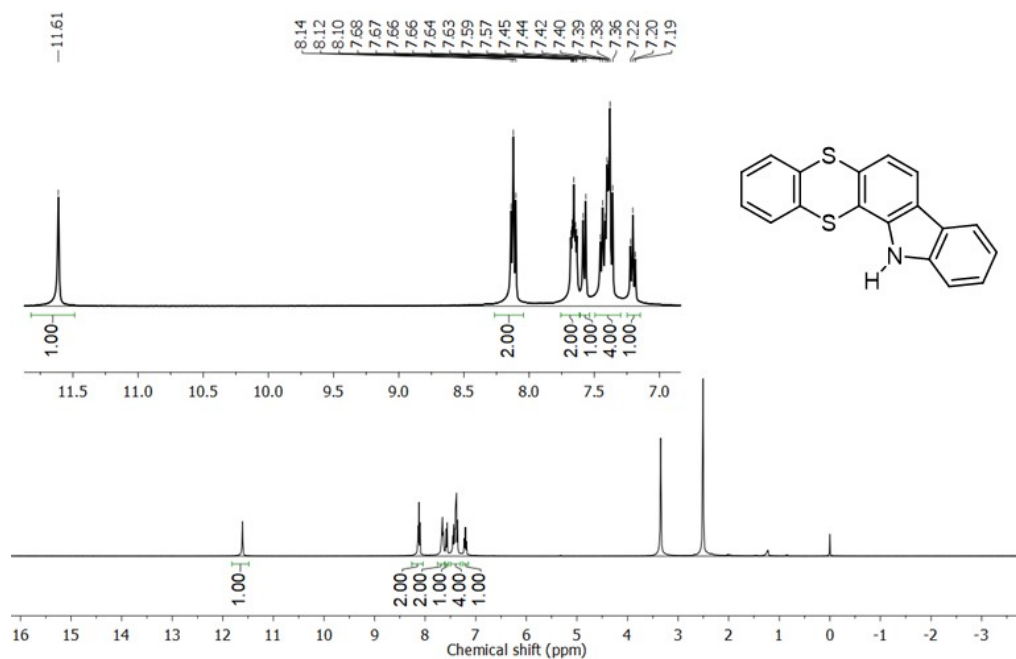




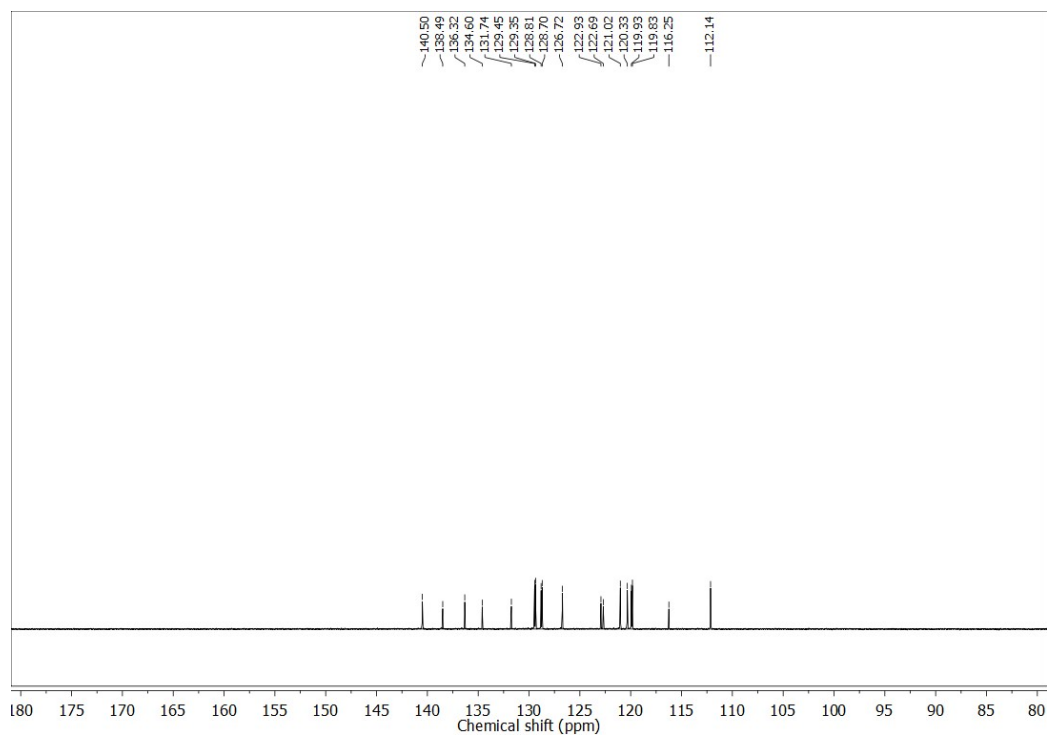
a) <sup>1</sup>H NMR spectrum of 5H-BOTCz in deuterated DMSO solvent.



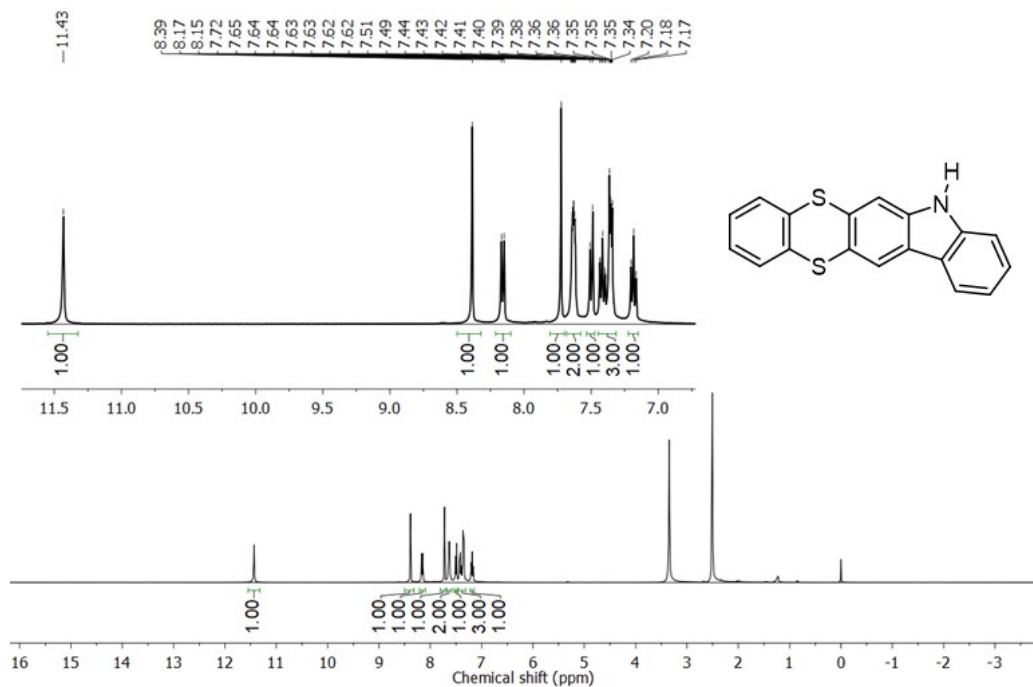
b) <sup>13</sup>C NMR spectrum of 5H-BOTCz in deuterated DMSO solvent.



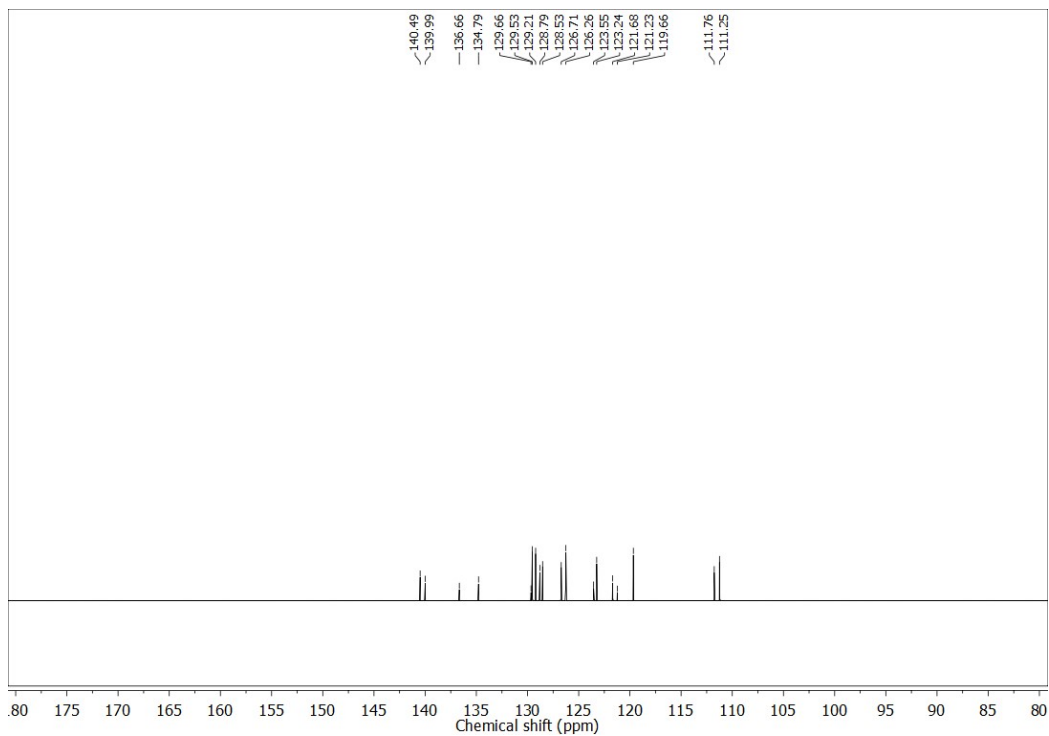
a) <sup>1</sup>H NMR spectrum of 12H-BDTCz in deuterated DMSO solvent.



b) <sup>13</sup>C NMR spectrum of 12H-BDTCz in deuterated DMSO solvent.



b) <sup>1</sup>H NMR spectrum of 5H-BDTCz in deuterated DMSO solvent.



b) <sup>13</sup>C NMR spectrum of 5H-BDTCz in deuterated DMSO solvent.

## 6. Reference

1. L. W. Chung, W. M. Sameera, R. Ramozzi, A. J. Page, M. Hatanaka, G. P. Petrova, T. V. Harris, X. Li, Z. Ke, F. Liu, H. B. Li, L. Ding and K. Morokuma, *Chem. Rev.*, 2015, **115**, 5678-5796.
2. K. Aidas, C. Angeli, K. L. Bak, V. Bakken, R. Bast, L. Boman, O. Christiansen, R. Cimraglia, S. Coriani, P. Dahle, E. K. Dalskov, U. Ekstrom, T. Enevoldsen, J. J. Eriksen, P. Ettenhuber, B. Fernandez, L. Ferrighi, H. Fliegl, L. Frediani, K. Hald, A. Halkier, C. Hattig, H. Heiberg, T. Helgaker, A. C. Hennum, H. Hettema, E. Hjertenaes, S. Host, I. M. Hoyvik, M. F. Iozzi, B. Jansik, H. J. Jensen, D. Jonsson, P. Jorgensen, J. Kauczor, S. Kirpekar, T. Kjaergaard, W. Klopper, S. Knecht, R. Kobayashi, H. Koch, J. Kongsted, A. Krapp, K. Kristensen, A. Ligabue, O. B. Lutnaes, J. I. Melo, K. V. Mikkelsen, R. H. Myhre, C. Neiss, C. B. Nielsen, P. Norman, J. Olsen, J. M. Olsen, A. Osted, M. J. Packer, F. Pawlowski, T. B. Pedersen, P. F. Provasi, S. Reine, Z. Rinkevicius, T. A. Ruden, K. Ruud, V. V. Rybkin, P. Salek, C. C. Samson, A. S. de Meras, T. Saue, S. P. Sauer, B. Schimmelpfennig, K. Sneskov, A. H. Steindal, K. O. Sylvester-Hvid, P. R. Taylor, A. M. Teale, E. I. Tellgren, D. P. Tew, A. J. Thorvaldsen, L. Thogersen, O. Vahtras, M. A. Watson, D. J. Wilson, M. Ziolkowski and H. Agren, *Wiley Interdiscip. Rev. Comput. Mol. Sci.*, 2014, **4**, 269-284.
3. B. Hess, C. Kutzner, D. van der Spoel and E. Lindahl, *J. Chem. Theory Comput.*, 2008, **4**, 435-447.
4. J. Wang, R. M. Wolf, J. W. Caldwell, P. A. Kollman and D. A. Case, *J. Comput. Chem.*, 2004, **25**, 1157-1174.
5. C. I. Bayly, P. Cieplak, W. Cornell and P. A. Kollman, *J. Phys. Chem.*, 1993, **97**, 10269-10280.